

X-ray absorption study of the electronic structure of Mn-doped amorphous Si

Li Zeng,^{1,a)} A. Huegel,¹ E. Helgren,¹ F. Hellman,¹ C. Piamonteze,² and E. Arenholz²

¹Department of Physics, University of California, Berkeley, Berkeley, California, 94720, USA

²Lawrence Berkeley National Laboratory, Advanced Light Source, Berkeley, California, 94720, USA

(Received 11 March 2008; accepted 20 March 2008; published online 8 April 2008)

The electronic structure of Mn in amorphous Si ($a\text{-Mn}_x\text{Si}_{1-x}$) is studied by x-ray absorption spectroscopy at the Mn $L_{3,2}$ edges for $x=0.005\text{--}0.18$. Except for the $x=0.005$ sample, which shows a slight signature of Mn^{2+} atomic multiplets associated with a local Mn moment, all samples have broad and featureless $L_{3,2}$ absorption peaks, corresponding to an itinerant state for all $3d$ electrons. The broad x-ray absorption spectra exclude the possibility of a localized $3d$ moment and explain the unexpectedly quenched Mn moment in this magnetically doped amorphous semiconductor. Such a fully delocalized d state of Mn dopant in Si has not been previously suggested. © 2008 American Institute of Physics. [DOI: 10.1063/1.2908050]

Mn is widely used as a magnetic dopant in diluted magnetic semiconductor (DMS) systems. The value of the Mn moment changes in different matrices due to different local environments. For Mn in crystalline Si ($c\text{-Si}$), both mean-field theory (Zener model) (Ref. 1) and first-principles calculations^{2,3} predict the presence of large Mn moments ($\geq 3\mu_B$) due to partially filled localized $3d$ levels. Experimentally, ferromagnetism is reported in Mn-doped crystalline group-IV semiconductors.^{4,5} However, homogeneous doping of Mn is difficult, largely due to the extremely low solubility of Mn ($x \sim 10^{-7}$) in crystalline group-IV semiconductors near room temperature.⁶ These issues were addressed by preparing Mn-doped Si in the amorphous form, enabling the study of the intrinsic Mn moment in the amorphous Si ($a\text{-Si}$) environment. Surprisingly, a quenched local Mn moment was observed by magnetic measurements.⁷

Ideal transition metal-doped ferromagnetic semiconductors rely on robust local moments associated with partially occupied $3d$ levels, which align via coupling through a low-density carrier system.⁸ Magnetization studies on Mn-doped $a\text{-Si}(a\text{-Mn}_x\text{Si}_{1-x})$ have shown that Mn in $a\text{-Si}$ has an unexpectedly small magnetization for the wide range of $x=0.005\text{--}0.18$. Even for the most dilute sample ($x=0.005$), the majority ($\sim 65\%$) of the Mn atoms are magnetically silent.⁷ This low magnetization can be a result of Mn low spin states, antiferromagnetic clusters, or the overlapping of $3d$ atomic orbitals resulting in a nonmagnetic band. With magnetic measurements alone, it is hard to distinguish between these alternative possible explanations.

In this letter, x-ray absorption spectroscopy (XAS) of Mn L edges is used to probe the $3d$ states of Mn in $a\text{-Si}$ by measuring the transition from occupied $2p$ core levels to the unoccupied $3d$ states. Since the magnetic states are closely related to the electronic structure, the local $3d$ moment can be deduced and compared to magnetization measurements. The measured Mn L edges have a very broad absorption feature, even at a very dilute Mn concentration (as low as $x=0.005$). The XAS results conclusively show that the d levels are fully extended into bands for doping concentrations x greater than 10^{-3} in $a\text{-Si}$, even for samples deep on

the insulating side of the insulator-metal ($I\text{-}M$) transition.

$a\text{-Mn}_x\text{Si}_{1-x}$ thin film samples were prepared by e-beam coevaporation of Mn and Si sources under ultrahigh vacuum conditions. High-resolution cross-sectional transmission electron microscopy with energy dispersive spectroscopy shows a homogeneous amorphous structure with no sign of any crystallinity, even at the nanoscale, and no sign of any Mn clustering. More detailed sample information can be found elsewhere.^{7,9} X-ray absorption (XA) and x-ray magnetic circular dichroism (XMCD) spectra at the Mn L edges were taken at the Advanced Light Source (ALS) beam line 6.3.1, in total electron yield mode. All measured thin film samples, including a control sample of a pure Mn metal film, were capped with 2–4 nm Al and stored in a vacuum desiccator to avoid oxidation. Commercially available Mn oxide powders with different Mn valences (MnO , Mn_2O_3 , and MnO_2 , corresponding to d^5 , d^4 , and d^3 configurations, respectively) were used as references.

Figure 1 shows the Mn $L_{3,2}$ spectra for all samples as well as a simulated Mn^{2+} spectrum. The atomic multiplet features of the Mn ion in different oxides can be well resolved. The spectra of the oxides are consistent with standard atomic multiplet simulations.¹⁰ We use the main Mn^{2+} L_3 absorption peak as our energy reference, which occurs at 639.0 eV in our data [Fig. 1(g); the feature at ~ 641.0 eV comes from Mn_2O_3 impurities in the MnO powder¹¹]. The XA spectra of $a\text{-Mn}_x\text{Si}_{1-x}$ [Figs. 1(a)–1(d)] have, in general, very broad L_3 and L_2 peaks, and no XMCD signal is observed in applied external fields up to 0.2 T at $T=8$ K, which is consistent with the lack of magnetization reported in Ref. 7. For $x \geq 0.04$, the spectra scale very well with x . The spectra of the sputtered Mn metal film and $a\text{-Mn}_x\text{Si}_{1-x}$ both show no distinct atomic multiplets, but they differ from each other in peak positions and peak widths: the main absorption peak of the Mn metal has a lower energy (639.4 versus 639.9 eV) and a narrower line width.

Figure 2 shows the detailed analysis of the L edges of $a\text{-Mn}_x\text{Si}_{1-x}$. For $x \geq 0.04$, the inset of Fig. 2 shows their collapse into a single curve after normalizing to the concentration-dependent postedge steps. The spectrum of the $x=0.005$ sample is normalized by the L_3 peak height since the signal/noise ratio is low at/beyond the L_2 -edge energy

^{a)}Electronic mail: li_zeng@berkeley.edu.

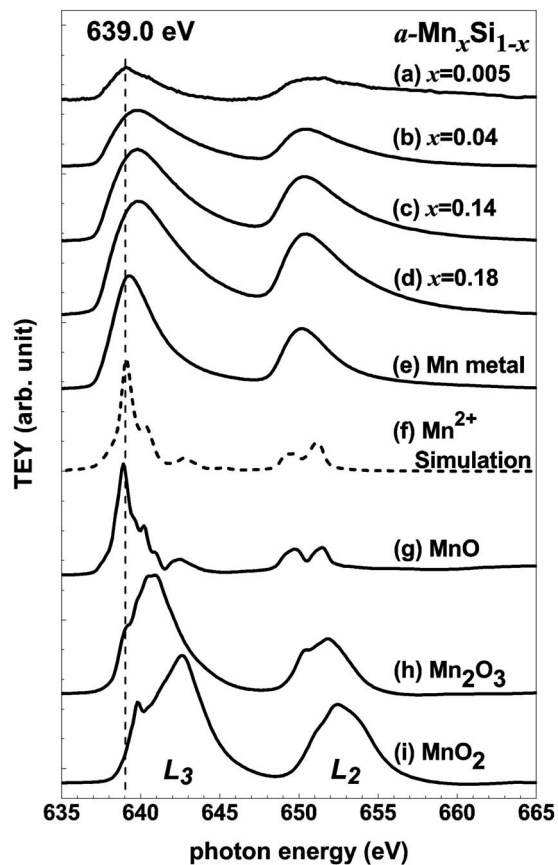


FIG. 1. XAS of the Mn L edges for the samples and standards. $a\text{-Mn}_x\text{Si}_{1-x}$ were prepared by e-beam coevaporation. The Mn metal film was prepared by magnetron sputtering at 4 mTorr, all at room temperature. All thin film samples were capped with 2–4nm Al. Mn oxides are commercially available chemicals powders. Compared to Ref. 11, both MnO and MnO₂ samples have an extra feature ~ 641.0 eV, indicating a small Mn³⁺ contribution.

due to the small Mn concentration. However, the $x=0.005$ sample obviously exhibits a different line shape at the L_3 edge with the L_3 peak at 639.0 eV, which is 0.9 eV lower in energy (with less broadening compared to the $x \geq 0.04$ samples) and aligned with the main Mn²⁺ L_3 peak, as marked with a dashed line in Fig. 1.

Besides the 639.0 eV peak, the L_3 edge of the $x=0.005$ sample also shows a broad shoulder at ~ 639.9 eV, which is an energy quite similar to the broad peak seen in all samples with $x \geq 0.04$. This strongly suggests that this spectrum consists of a mixture of a Mn²⁺ multiplet and another broad XA peak centered at ~ 639.9 eV, which is most likely the Mn XA spectra observed in the $x \geq 0.04$ samples. We test this idea by performing a weighted superposition of the broad spectrum of $x=0.18$ [Fig. 3(a)] and the Mn²⁺ spectrum [Fig. 3(d)] to match the measured spectrum for the $x=0.005$ sample [Fig. 3(c)] at the L_3 edge. The simulated spectrum [Fig. 3(b)] reproduces the features of the $x=0.005$ sample's spectrum well. The broad absorption peak found in high Mn doping samples develops even at a Mn concentration as low as $x=0.005$, with a significant fraction ($>60\%$) of the incorporated Mn, which is reminiscent of the nonmagnetic Mn portion ($\sim 65\%$) found in a similar low Mn concentration in the previous magnetization study. These results link the broad XA spectra with the nonmagnetic Mn state. The consistency between the XA data and the magnetization results

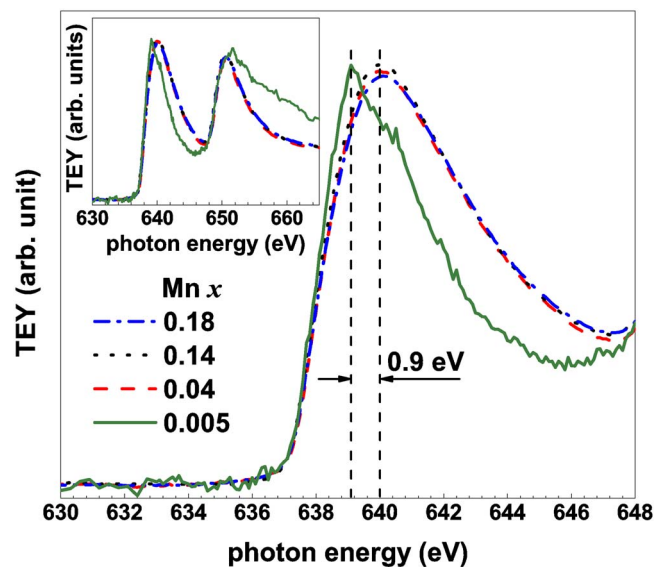


FIG. 2. (Color online) L_3 edges of all $a\text{-Mn}_x\text{Si}_{1-x}$ samples. Spectra were normalized to the L_3 peak height to illuminate the differences in peak positions and peak widths. Inset: The Normalized spectra (described in the text) show how the overall spectrum shapes of both L_3 and L_2 scale with x for $x=0.04$, 0.14, and 0.18 but do not scale for $x=0.005$.

strengthens the two-state model we proposed for $a\text{-Mn}_x\text{Si}_{1-x}$.⁷

The surprising nonmagnetic states seen in $a\text{-Mn}_x\text{Si}_{1-x}$ thus seem to be associated with the broad XA spectra seen here and strongly argues against Mn ions with a low spin state, or atomic force microscopy (AFM) coupled Mn moments because in either case, the XA spectra would have shown multiplet structures. Moreover, a large crystal field (CF) splitting is a prerequisite for low spin states, but CF splitting is a small effect in Si, as stated by the Ludwig–Woodbury model.¹² Disorder in $a\text{-Si}$ would introduce randomness in the CF strength. We therefore performed multiplet simulations with varying CF strengths. The CF of Mn oxides was used as an upper bound of the CF strength in Si, which is found to be ≤ 2 eV (for Mn⁴⁺ in MnO₂) according to our simulations. A varying CF between 0 and 2 eV pro-

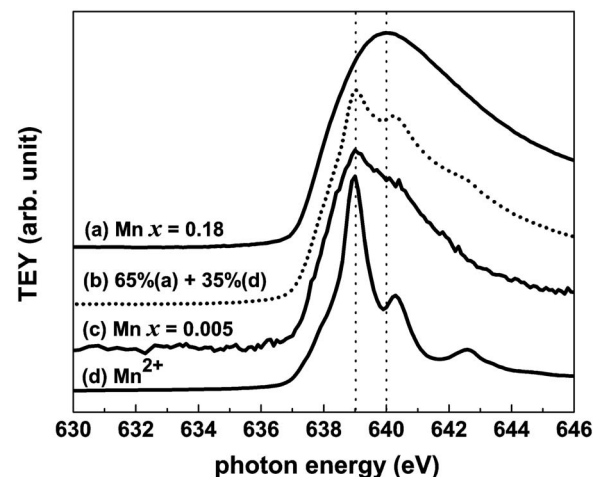


FIG. 3. Demonstration of the existence of mixed states in the $x=0.005$ sample [curve (c)] by superposition of the calculated L_3 edge of Mn²⁺ [curve (d)] and of the $x=0.18$ sample [curve (a)]. The dashed-dotted curve (b) is the best match to curve (c). The uncertainty in the spectral weight of curves (a) and (d) is $\sim 10\%$.

duces small effects (~ 0.5 eV shift) on the main L peak. Thus, even if a random distribution of CF strengths exists due to disorder, linear combinations of the corresponding weighted spectra would not yield the observed smooth and broad XA peaks (full width at half maximum ~ 5 eV).

Mixed Mn valence states can lead to a significant XA broadening, such as found in (La,Ca)MnO₃ (LCMO) and MnSi crystalline compounds. In LCMO, the L -edge broadening is due to the coexistence of Mn³⁺ and Mn⁴⁺ sites,¹³ and in crystalline MnSi, it is proposed to be the mixed-valence ground state, which consists of different d multiplets.¹⁴ However, the underlying features from the atomic multiplets are still clearly visible in those spectra.

In a p - d hybridization scenario, as for the well-studied FM Mn-doped III-V DMS systems, multiplet structures are compressed and shifted due to the charge transfer effect and screening.¹¹ This leads to narrower L peaks and a peak shift of 0.5 eV to a lower energy,^{15,16} in contrast to what we have observed for the a -Mn _{x} Si_{1- x} samples, where peaks are broader and shifted 0.9 eV higher in energy. Covalency of Mn-Si bonds is expected to be even stronger than that of Mn-As bonds and, thus, cannot account for the observed XA spectra broadening and shift. Moreover, hybridized but still localized $3d$ levels should still possess large local Mn moments, which would have been detected by magnetization measurements.¹⁶

We propose instead that the smooth broad L edges of a -Mn _{x} Si_{1- x} are most likely due to the formation of an itinerant impurity band of the $3d$ electrons. Mn metallic clusters are excluded by previous materials characterization.⁷ The atomic density obtained from Rutherford backscattering and film thickness measurements linearly increases with Mn doping x , suggesting that Mn are at interstitial-like positions with high Si coordination numbers, as in other crystalline MnSi silicides.^{14,17} The Mn centers and Mn-Si covalent bonds can lead to delocalized states and the formation of an itinerant impurity band. Moments associated with metallic bands are usually small, if present at all, such as in the Mn₄Si₇ silicide and the itinerant helimagnet MnSi.^{14,18} The existence of a well defined band with the electrons being localized due to disorder in these insulating samples (defined as vanishing conductivity at $T \rightarrow 0$ K in I - M transition physics; $x=0.005$ and 0.04 samples are on the insulating side) is consistent with the Anderson localization theory.¹⁹ Furthermore, the formation of a band by the Mn $3d$ electrons, perhaps as a hybridization with Si s or p electrons, is possible without long-range order and explains the broad shape of the XA spectra. Also, the evidence of a well defined band in this system can be viewed as a precursor to the MnSi helimagnet with the disorder breaking the long-range order needed for a true magnetic ground state.

In conclusion, we have demonstrated that the XAS of a -Mn _{x} Si_{1- x} for $x=0.005$ – 0.18 can be modeled by a superposition of two distinct electronic states that are associated with a small fraction of Mn²⁺ magnetic states and a dominant Mn nonmagnetic state, which is in good agreement with previous magnetization data. The L edges corresponding to the nonmagnetic states have very broad and smooth absorption peaks, which argues against the existence of Mn low spin states and AFM clusters. Instead, the broad XA spectra are evidence of a fully delocalized d state and the formation of impurity bands, which explain the absence of magnetic Mn in the a -Si matrix previously observed.

We thank E. Cruz and D. R. Queen for assistance. Synthesis was supported by NSF DMR-0505524 and measurements were supported by DOE Division of Materials Sciences and Engineering under Contract No. DE-AC02-05CH11231. The Advanced Light Source is supported by the Director, Office of Science, Office of Basic Energy Sciences, of the U.S. Department of Energy under Contract No. DE-AC02-05CH11231.

¹T. Dietl, H. Ohno, F. Matsukura, J. Cibert, and D. Ferrand, *Science* **287**, 1019 (1998).

²A. Stroppa, S. Picozzi, A. Continenza, and A. J. Freeman, *Phys. Rev. B* **68**, 155203 (2003).

³F. Bernardini, S. Picozzi, and A. Continenza, *Appl. Phys. Lett.* **84**, 2289 (2004).

⁴Y. D. Park, A. T. Hanbicki, S. C. Erwin, C. S. Hellberg, J. M. Sullivan, J. E. Mattson, T. F. Ambrose, A. Wilson, G. Spanos, and B. T. Jonker, *Science* **295**, 651 (2002).

⁵M. Bolduc, C. Awo-Affouda, A. Stollenwerk, M. B. Huang, F. G. Ramos, G. Agnello, and V. P. LaBella, *Phys. Rev. B* **71**, 033302 (2005).

⁶E. R. Weber, *Appl. Phys. A: Solids Surf.* **30**, 1 (1983).

⁷L. Zeng, E. Helgren, M. Rahimi, F. Hellman, R. Islam, B. J. Wilkens, R. J. Culbertson, and D. J. Smith, *Phys. Rev. B* **77**, 073306 (2008).

⁸A. H. MacDonald, P. Schiffer, and N. Samarth, *Nat. Mater.* **4**, 195 (2005).

⁹L. Zeng, E. Helgren, F. Hellman, R. Islam, and D. J. Smith, *Phys. Rev. B* **75**, 184404 (2007).

¹⁰F. M. F. de Groot, *Chem. Rev. (Washington, D.C.)* **101**, 1779 (2001).

¹¹F. M. F. de Groot, *J. Electron Spectrosc. Relat. Phenom.* **67**, 529 (1994).

¹²G. W. Ludwig and H. H. Woodbury, *Phys. Rev. Lett.* **5**, 98 (1960).

¹³S. Valencia, A. Gaupp, W. Gudat, L. Abad, L. Balcells, A. Cavallaro, B. Martínez, and F. J. Palomares, *Phys. Rev. B* **73**, 104402 (2006).

¹⁴F. Carbone, M. Zangrando, A. Brinkman, A. Nicolaou, F. Bondino, E. Magnano, A. A. Nugroho, F. Parmigiani, T. Jarlborg, and D. van der Marel, *Phys. Rev. B* **73**, 085114 (2006).

¹⁵K. W. Edmonds, N. R. S. Farley, T. K. Johal, G. van der Laan, R. P. Campion, B. L. Gallagher, and C. T. Foxon, *Phys. Rev. B* **71**, 064418 (2005).

¹⁶P. R. Stone, M. A. Scarpulla, R. Farshchi, I. D. Sharp, E. E. Haller, O. D. Dubon, K. M. Yu, J. W. Beeman, E. Arenholz, J. D. Denlinger, *Appl. Phys. Lett.* **89**, 012504 (2006).

¹⁷H. W. Knott, M. H. Mueller, and L. Heaton, *Acta Crystallogr.* **23**, 549 (1967).

¹⁸U. Gottlieb, A. Sulpice, B. Lambert-Andron, and O. Laborde, *J. Alloys Compd.* **361**, 13 (2003).

¹⁹P. W. Anderson, *Phys. Rev.* **124**, 41 (1961).